Local correlation of low-SNR and strongly RFI contaminated DOR signals

Maoli Ma[1,3], Peijia Li[1], Fengxian Tong[1,3], Weimin Zheng[1,2,3], Tetsuro Kondo[1], Lei Liu[1,3], Xiaojing Wu[1], Xin Zheng[1,3]

[1]Shanghai Astronomical Observatory, Chinese Academy of Science
[2]Shanghai Key Laboratory of Space Navigation and Positioning Techniques,Shanghai Astronomical Observatory, Chinese Academy of Sciences
[3]Shanghai Astronomical Observatory, Chinese Academy of Sciences, Key Laboratory of Radio Astronomy, Chinese Academy of Sciences
[1]Shanghai 200030,China
[2]Shanghai 200030,China
[3]West Beijing Road, Nanjing, Jiangsu 210008, China

Key Points:

- Delta-DOR
- China VLBI net
- Longjiang 2
- Chang' E 3

Corresponding author: Weimin Zheng, zhwm@shao.ac.cn

Corresponding author: Maoli Ma, mamaoli@shao.ac.cn

Abstract

This paper presents the local correlation method of low-SNR (Signal to Noise Ratio) and strongly RFI (Radio Frequency Interference) contaminated DOR (differential one-way ranging) signals with China's lunar spacecraft. Unlike the Very Long Baseline Interferometry (VLBI) FX correlator used in China VLBI net, the core of local correlation is to construct the received signal model based on the intrinsic characteristics of DOR signals, then extract the residual frequency and phase relative to the model. The performance of the method is verified by means of orbit determination and post-fit residuals analysis. The RMS (root-mean-square) of Delta-DOR delay after orbit determination are 3.7 ns and 0.83 ns when tones SNR varied of 1 dBHz $\sim$ 20 dBHz and 14 dBHz $\sim$ 26 dBHz in two individual experiments. The computed standard deviation of post-fit delay residuals is compatible at 3 sigma level with the theoretical spacecraft thermal noise. Local correlation provides a solution to the special RFI contaminated DOR signals process. The precision of Delta-DOR delay with strong RFI keeps the same level of that without interference.

1 Introduction

Very Long Baseline Interferometry (VLBI) is a technique that can determine the angular position of distant radio sources by measuring the geometric time delay between the received radio signals at geographically separated stations. Delta Differential One-way Ranging (Delta-DOR) originally developed by Jet Propulsion Laboratory in the late 1970 (Curkendall & Border, 2013) is a navigation application of VLBI. It can be used in conjunction with Doppler and ranging data to determine the spacecraft angular position in the celestial sphere efficiently.

Delta-DOR is generally conducted by deep space navigation stations, including Goldstone, Madrid, Canberra for National Aeronautics and Space Administration (NASA) (Border, 2014), and Cebreros, New Norcia, Malargue for European Space Agency (ESA) (James et al., 2009). The tracking data are transferred to data processing center for correlation. As a kind of artificial signal, DOR signals which consist of a series of intrinsic narrowness tones or harmonics of the existing telemetry subcarriers are different from the wideband noise-like signal radiated from quasars. NASA had developed a special software correlator package for Delta-DOR Navigation processing (Rogstad et al., 2009). ESA had developed its own correlator with jointly cooperation with University of Rome "La Sapienza" (Iess & Ardito, 2006).

Delta-DOR has been extensively and successfully applied to a lot of deep-space missions. Among these missions there are Mars Observer, Mars Odyssey, Phoenix, MAVEN (Curkendall & Border, 2013) (Kinman et al., 2015), etc. Different agencies have established cooperation and inter-operability for cross support of space missions. Tracking data can be exchanged under the conventions and definitions of Delta-DOR in Consultative Committee for Space Data Systems (CCSDS, 2013).

China's Lunar Exploration Project (CLEP) has utilized VLBI stations to support Delta-DOR measurement since Chang' E 3 in 2013 (W. Wu et al., 2013). Chinese VLBI net (CVN) including BJ (50 m), KM (40 m), UR (26 m), TM (65 m) has carried out the observations and transferred tracking data to VLBI center for correlation. The CVN correlator is FX (Fourier transform and cross multiplication) type VLBI correlator (Zheng et al., 2014). The measurement accuracy and real-time ability are better than the requirements of the missions.

During the Chang' E observations, CVN encountered with some low-SNR (Signal-to-noise Ratio) or strongly RFI (Radio Frequency Interference) contaminated DOR signals. An increasement of FFT (Fast Fourier Transform) points is required for FX correlator to distinguish the low-SNR intrinsic narrowness tones. The strong RFI was data-transmission signal emitted from another transponder on the same spacecraft. When the two different transponders on Chang'E 3 emitting DOR signals and data-transmission signal meanwhile, DOR signals will be strongly contaminated by the side lobes of the data-transmission signal. The increasement of FFT points sometimes can't distinguish tones if they are totally

submerged in the strong RFI.
In this paper, we propose a different local correlation method to process the low-SNR and strongly RFI contaminated DOR signals. In section 2 we describe DOR signals and its characteristics. Section 3 describes correlation methods. Section 4 describes the DOR experiments setting. Section 5 describes correlation applications in experiments. Section 6 is results and analysis. Section 7 is conclusions.

2 DOR signals

In CLEP, X-band DOR is used in Chang'E 3, Chang'E 4 and Chang'E 5. S-band DOR is used in lunar microsatellite Longjiang and Chang'E 4 relay satellite Queqiao. The DOR tones are generated from modulation by sine waves on the downlink carrier signal. X-band DOR is expressed as follow (CCSDS, 2013),

$$\begin{aligned} s(t) =& \sqrt{2P_T}[J_0(m_1)J_0(m_2)\cos(2\pi f_c t) - 2J_1(m_1)J_0(m_2)\sin(2\pi f_c t)\sin(2\pi f_1 t) \\ & - 2J_0(m_1)J_1(m_2)\sin(2\pi f_c t)\sin(2\pi f_2 t) + higher\ harmonics] \end{aligned} \tag{1}$$

P_T is the total power of downlink signal. f_c is the frequency of the main carrier. f_1 and f_2 are phase modulation frequency. $f_{1,2}$ has a relationship with f_c, $f_{1,2}/f_c = n_{1,2}$, where $n_{1,2}$ are frequency modulation indices. m_1 and m_2 are amplitude modulation indices. J_0 and J_1 are Bessel functions of the first kind.
Fig.1 shows X-band DOR signals. The modulation produces a pair of narrow spanned bandwidth tones f_{R1}, f_{L1} with frequency separation 7.6 MHz and wider spanned bandwidth tones f_{R2}, f_{L2} with frequency separation 38.4 MHz. f_{R1}, f_{L1} are provided for integer cycle phase ambiguity resolution. f_{R2} and f_{L2} with wider frequency separation are used to determine delay observables.
Amplitude modulation indices m_1 and m_2 decide the power allocation between the carrier

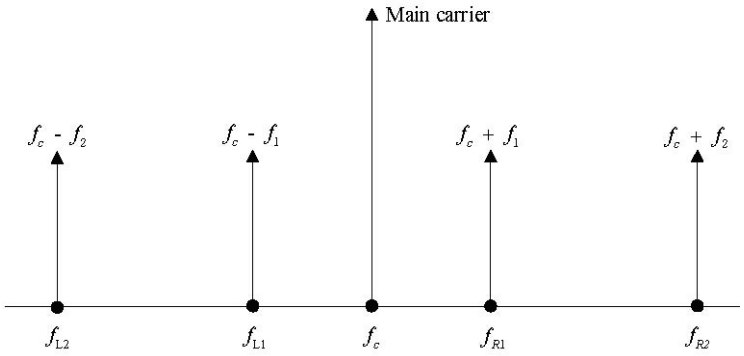

Figure 1. X-band DOR signals. The tones are generated from modulation on the downlink carrier signal. f_c is the main carrier, f_{R1} and f_{L1} are narrow spanned bandwidth tones, f_{R2} and f_{L2} are wider spanned bandwidth tones.

and the tones, where

$$\begin{aligned} P_c &= P_T J_0^2(m_1) J_0^2(m_2) \\ P_{R1/L1} &= P_T J_1^2(m_1) J_0^2(m_2) \\ P_{R2/L2} &= P_T J_0^2(m_1) J_1^2(m_2) \end{aligned} \tag{2}$$

In Chang' E spacecraft, the nominal values of the DOR modulation indices are $m_1 = m_2 =$ 0.4 rad. Such values yield modulation losses P_c/P_T=-0.7 dB, $P_{R1/L1}/P_T = P_{R2/L2}/P_T$

=-14.5 dB. Therefore tones are -13.8 dB weaker than the main carrier. The S-band DOR in Longjiang 2 and Queqiao only has one pair of tones with spanned bandwidth of 7.6 MHz. The modulation losses of tones are same as that of X-band DOR.
From Equation (1) and (2), one can find that a series of intrinsic narrow single-frequency lines comprise of the DOR signals. The tones are coherently related to the main carrier even under the lower SNR cases. So we can make use of carrier-aid method on tones to extract the residual frequency and phase of tones when they're seriously interfered.

3 Local correlation algorithm

Fig.2 shows the DOR tracking geometry of a spacecraft. In the geocentric coordinate system, **E** is the geocentric center, **Sc** is the spacecraft. **A** and **B** are two VLBI antennas. The position vector of spacecraft and **A**, **B** are $\mathbf{r_{Sc}(t)}$, $\mathbf{r_A(t)}$ and $\mathbf{r_B(t)}$.
In CVN FX correlator, the signals from each antenna should be time-shifting to the geocen-

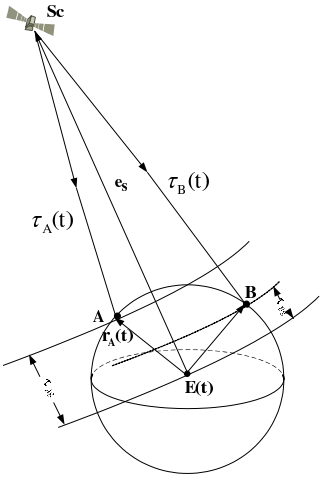

Figure 2. DOR tracking geometry of a spacecraft, and the different models used in VLBI FX correlator and local correlation. $\tau_{Ag}(t)$ and $\tau_{Bg}(t)$ are used by FX correlator for time-shifting the signal from topocentric to geocentric frame. $\tau_A(t)$ and $\tau_B(t)$ are used by local correlation for eliminating Doppler shift.

tric frame such that all signals track the same wave front. A near-field delay model is used for spacecraft delay compensation, shown as $\tau_{Ag}(t)$ and $\tau_{Bg}(t)$ in Fig.2. Cross-correlation is carried on the frequency domain after FFT on signals. An SNR loss due to the frequency smearing and spectrum leakage is given by $-10log_{10}\sqrt{\frac{BW}{N}}$, where N is FFT points and BW is bandwidth (Liu et al., 2015). The typical values of BW and N used in CVN FX correlator are BW = 2 MHz and N = 8192. It leads to a SNR loss of -11.9 dB. To distinguish tones with intrinsic narrowness, FX correlator need a large number of FFT points. Duev et al. (2016) used different spectral resolution to correlate the individual sub-carrier lines of Mars Express on several baselines. The fringe-fitting results suggested an optimal spectral resolution value of $N = 2^{19} = 524288$ points for the intrinsic narrow lines when BW = 16 MHz.
Fig.3 is the local DOR correlation flowchart. The core of local correlation is to construct a received signal model to eliminate Doppler effect and extract residual frequency and phase of DOR signals relative to the model signal. Instead of $\tau_{Ag}(t)$ and $\tau_{Bg}(t)$ used in FX correlator, local DOR correlation compensates earth rotation and the spacecraft motion with the reconstructed model signals $s_A(t)$ and $s_B(t)$, which derived from the dynamical light time model $\tau_A(t)$, $\tau_B(t)$ and transmit frequency f_t of main carrier.

$$s_{A,B}(t) = \exp[j2\pi f_t(t - \tau_{A,B})] \tag{3}$$

$\tau_A(t)$ and $\tau_B(t)$ are derived from a prior spacecraft ephemerides and the relative motion between the spacecraft and the stations. In the typical Delta-DOR sessions for Chang' E spacecraft, the telecommunication link is configured in a three-way mode, with the emitted signal generated by the uplink station. Both uplink and downlink light travel paths are considered in $\tau_A(t)$ and $\tau_B(t)$.

The reconstructed model signals are then mixed with real signals. This step compensates a large amount of frequency variation caused by the Doppler shift. The small residual frequency offsets usually less than 1 Hz are mainly from a priori uncertainties of the spacecraft ephemerides.

The mixed signals are then filtered to remove high frequency components, and conjugate multiplied together to generate $X_{AB}(t)$. $X_{AB}(t)$ can be modeled as

$$X_{AB}(t) = \exp[j2\pi f_{AB}t + j\phi_{AB})] + noise \tag{4}$$

Where f_{AB} and ϕ_{AB} are the residual frequency and phase between A and B. The residual phase ϕ_{AB} of other tones could be obtained in the similar method.

Theoretically, DOR delay depends only on the geometry of the measurement system. However, the delay are still biased by ground station clock offsets, instrumental delays, propagation media (especially troposphere and ionosphere) effects, etc. In order to minimize the bias, a nearby extragalactic quasar should be selected as a calibrator. The separation angle between quasar and spacecraft is usually less than 10°. In general, Delta-DOR takes an alternative observation sequence like quasar-spacecraft-quasar or spacecraft-quasar-spacecraft. The residual phase from quasar observation is used to calibrate the common error of ϕ_{AB}. Then we obtain $\Delta\tau$ through a bandwidth synthesis technique. $\Delta\tau$ accounts for the deviation of measured observables to the computed model delay. The measured Delta-DOR delay τ_{sc} is

$$\tau_{sc} = \tau_B - \tau_A + \Delta\tau \tag{5}$$

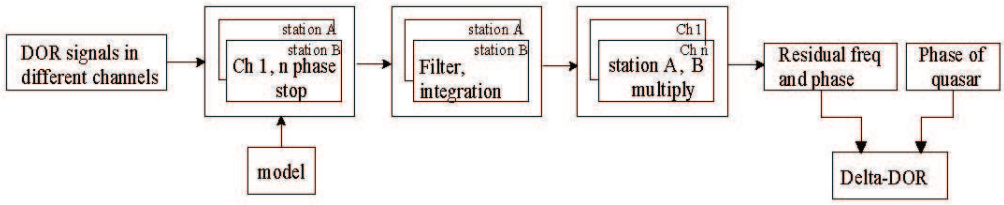

Figure 3. DOR correlation flowchart

4 Observations

CVN has conducted hundreds of Delta-DOR observations of Chang' E spacecraft. The down-converted radio signal is recorded using CDAS (Chinese VLBI Data Acquisition System) terminals (Y. Wu, 2009). The main carrier and individual tones are usually recorded with 8 or 16 frequency channels, with 2 or 4 MHz bandwidth and two-bit encoding. The data collected at different stations are then transferred to the VLBI center for correlation. Generally, the SNR of DOR signals of Chang' E spacecraft is very strong. The nominal value of P_c/N_0 (main carrier power-to-noise ratio) is about 45 dBHz, P_{tone}/N_0 (tone power-to-noise ratio) 35 dBHz. A spectral resolution of several hundred Hz is sufficient for a FX

correlator to extract the residual frequency and phase of tones.

The observations of low-SNR and strongly RFI contaminated Delta-DOR experiments are presented in Table 1. S8525b and s8524b are observations for relay spacecraft Queqiao and microsatellites Longjiang 2. Longjiang 2 was lunched accompany with Queqiao on 21th, May 2018, but kept some angle separations during the cruise stage. The two spacecraft were observed in the same beam of VLBI antennas until their completely separation on 25th, May 2018, on which date Queqiao transferred to an eventual Langrange 2 Halo orbit, and Longjiang 2 was set into an elliptical lunar orbit. VLBI antennas pointed to Queqiao and brought in a pointing deviation to Longiang 2. The pointing-off of antennas to Longjiang 2 lead to the lower SNR signals compared with Queqiao. The half power beam width of BJ, KM, UR and TM antennas are 0.15°, 0.19°, 0.3° and 0.12° respectively. In s8525b, Longjiang 2 was out of the half power beam width. The maximum offset from pointing was up to 0.6°.

Longjiang 2 emitted signals at S-band (∼2.2GHz). The P_c/N_0 of main carrier of Longjiang

Table 1. Experiments of DOR correlation

code	data	spacecraft	band	stations	length of time
*s*8525*b*	2018-05-25	Longjiang-2	S-band	BJ,KM,UR,TM	4 hours
*s*8524*b*	2018-05-24	Longjiang-2	S-band	BJ,KM,UR,TM	2.9 hours
*s*7912*a*	2017-09-12	Chang'E 3 lander	X-band	SH,KM,UR	1.4 hours

[a]Footnote text here.

2 in s8524b and s8525b are presented in Fig.4. The P_c/N_0 performance for VLBI stations are significantly different because of the different pointing deviation to spacecraft. The P_c/N_0 of main carrier in s8525b varies from 15 dBHz ∼ 40 dBHz. It means 1 dBHz ∼ 25 dBHz for P_{tone}/N_0 derived from Equation (2). P_c/N_0 in s8524b is stronger than those of s8525b with minimum 10 dBHz for P_{tone}/N_0.

S7912a is a Chang'E 3 lander observation. Chang'E 3 was soft landed on the Moon in

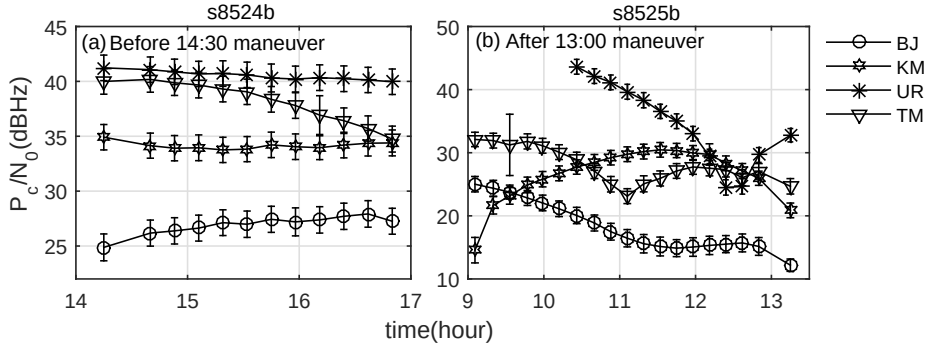

Figure 4. P_c/N_0 of Longjiang-2 DOR main carrier in s8524b and s8525b. Ur didn't attend spacecraft observation until 10:23 because of low elevation in s8525b.

the east of Sinus Iridum area on 14, Dec. 2013 (Zheng et al., 2017). It can transmit both DOR signals and data-transmission signal. In s7912a, when two kinds of signals transmitted at the same time, DOR signals were seriously interfered by the data-transmission signal. Fig.5 are power density spectrums of tones and data-transmission signal. P/N_0 of carrier and tones are 48.2 dBHz, 37.6 dBHz, 34.5 dBHz, 34 dBHz and 35.2 dBHz, respectively.

Compared with f_{L2}, f_{R2} is seriously interfered by the side lobe of data-transmission signal. Other tones are also contaminated by data-transmission signal to different degree.

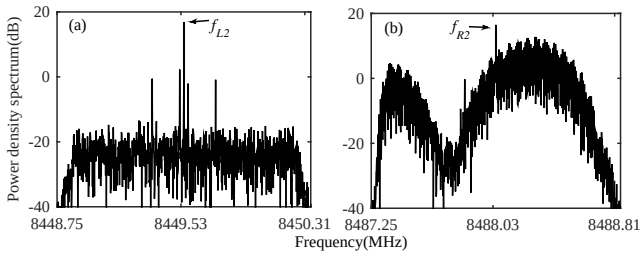

Figure 5. Power density spectrum of DOR tones and data-transmission signal from Chang'E 3 lander. Integration time is 5 s, spectral resolution is 2 KHz, sample rate is 4 MHz, bandwidth is 2 MHz, quantification is 2 bit. Comparing with f_{L2}, f_{R2} is serious interfered by data-transmission signal.

5 Local correlation on experiments

5.1 Local correlation

We have completed the spacecraft data processing on the above low-SNR and strongly RFI contaminated DOR signals. Fig.6 shows the power density spectrum for the main carrier and the tone of BJ station in s8525b. P_c/N_0 is 16.5 dBHz, P_{tone}/N_0 2.5 dBHz derived from the amplitude modulation indices (Equation 2). Tones were totally submerged in noise. Transmit frequency from uplink station and the light time model were used to construct a received signal model for phase stopping. After the phase stopping, the frequency of the signal becomes to be nearly zero. We filtered out the undesired high frequency components outside a selectable bandwidth through integration. The filter bandwidth was 20 Hz. P_{tone}/N_0 and P_c/N_0 increase to 13 dBHz and 30 dBHz respectively after phase stopping and integration (Fig.6). The method was limited to detect tones for BJ station after UTC 13:00 when P_c/N_0 was below 15 dBHz.

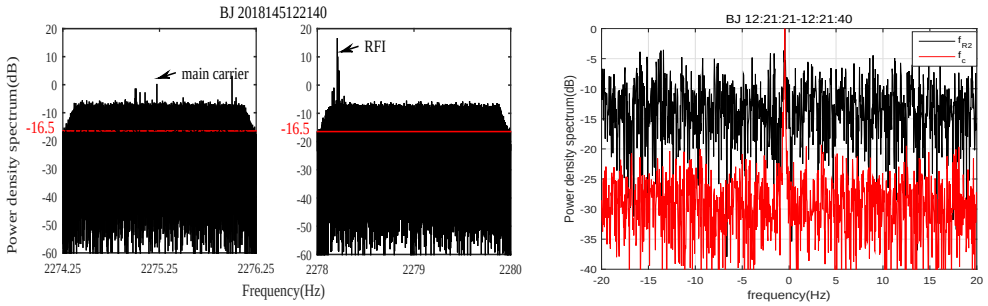

Figure 6. Power density spectrum of the main carrier and the tone in BJ. Left: Spectrums of raw data, integration time is 1 s. The red lines are noise density. P_c/N_0 is 16.5 dBHz. The tone is totally submerged in the noise. Right: Spectrums after phase stop and integration, integration time is 20 s. P_{tone}/N_0 and P_c/N_0 increase to 13 dBHz and 30 dBHz respectively.

Correlation for s7912a with strong RFI is a little different from the low-SNR signal process. The strong main carriers with P_c/N_0 48 dBHz in s7912a allowed us to use the carrier-aid method. A digital Phase Lock Loop (PLL) was used on the main carrier to filter out undesired interfering data-transmission signal outside a selectable bandwidth. Then phase from PLL was used to track tones with serious interference.
In order to evaluate data-transmission signal' s affection on tones, we used a three-order polynomial to fit frequency and phase at each independent scan, then calculated standard variance (STD) of the residual frequency and phase corresponding to the phase model from PLL. The results are presented in Table 2. Although f_{R2} is seriously contaminated by data-transmission signal in s7912a, σ_f and σ_φ for those tones are statistically compatible with main carrier or other slight contaminated tones. The interfering data-transmission signal is effectively filtered out after correlation.

Table 2. Standard variance of residuals frequency and phase in s7912a. σ_f : mHz, σ_φ : degree

baseline	f_{L2} $\sigma_f,\ \sigma_\varphi$	f_{L1} $\sigma_f,\ \sigma_\varphi$	f_{R1} $\sigma_f,\ \sigma_\varphi$	f_{R2} $\sigma_f,\ \sigma_\varphi$
SH-KM	1.4, 1.7	1.4, 1.7	1.5, 2.3	1.5, 2.3
SH-UR	0.7, 0.6	0.6, 0.6	0.6, 0.6	0.7, 0.6
KM-UR	1.3, 1.7	1.3, 1.7	1.3, 1.7	1.3, 1.7

5.2 Bandwidth synthesis

To get the Delta-DOR delay, bandwidth synthesis was performed on tones. The tones were recorded at different frequency channels, the strong fringe find quasars were used to calibrate the initial instrument phase error. Then the reference quasars were used to calibrate the common error from the atmosphere, ionosphere, instrument, station position error.
After calibration, we used the inner DOR tones to solve the 2π phase ambiguity. If the frequency interval between inner tones is Δf, the corresponding delay ambiguity is $\tau_a = 1/\Delta f$, distance between spacecraft and earth is l, the longest length of baseline projection onto plane-of-sky is d, the delay deviation caused by prior orbit deviation is $\tau^p = \Delta d \cdot d/(\upsilon_c \cdot l) * 10^9$ ns, υ_c is the velocity of light. For CVN VLBI stations, d is about 3000 km.
S8524b carried out the orbit insertion maneuver before 14:30. The prior ephemerides used for correlation was the initial orbit before maneuvering. The prior orbit deviation was 10 km. It led to a nearly 270 ns delay offset, larger than the delay ambiguity of S-band DOR, which is 125 ns. We used an even harmonic of the telemetry subcarriers with spanned bandwidth 1 MHz as well to solve phase ambiguity. The delay ambiguity determined by subcarriers was 1000 ns, larger than the delay deviation caused by the inaccurate prior orbit. Fig.7 are the residual Delta-DOR delay in s8524b and s8525b. Delta-DOR delay in s7912a was obtained by the same method.

6 Results and analysis

The validation of the local correlation method of the low-SNR and strongly RFI contaminated DOR has been carried out by the post-fit or orbit determination on measurements. We took a third order polynomial fit on the residual delay, the computed STD of residuals at different baselines are represented in Table 3. The expected spacecraft thermal noise $\varepsilon_{\tau_{SC}}$ was estimated from P_{tone}/N_0 and spanned bandwidth f_{BW} (Kinman et al., 2015).

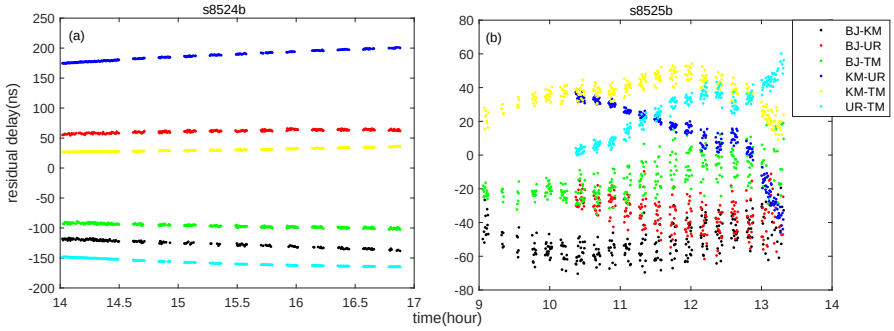

Figure 7. Residual delay from s8524b and s8525b

$$\varepsilon_{\tau_{SC}} = [(\frac{\sqrt{2}}{2\pi f_{BW}} \frac{1}{SNR_1})^2 + (\frac{\sqrt{2}}{2\pi f_{BW}} \frac{1}{SNR_2})^2]^{1/2}\mathrm{s} \tag{6}$$

The SNR_i for tones at station i is given by

$$SNR_i = \sqrt{2(P_{tone}/N_0)_i T_{SC}} \tag{7}$$

T_{SC} is the integration time. f_{BW} is about 7.6 MHz for S-band DOR, 38.4 MHz for X-band DOR. P_{tone}/N_0 of different stations was estimated from Fig. 4 and Equation (2). Table 2 shows that the result of computed STD is compatible at 3 sigma level with the expected spacecraft thermal noise.

The unified X-band range and Delta-DOR were combined and applied in orbit determination. The range in s8525b and s8524b were from Qingdao (18 m) and Jiamusi (66 m) respectively. The observables after 13:00 in s8525b or before 14:30 in s8524b were excluded because the spacecraft performing orbit insertion maneuver. No quasar was observed during these periods. The RMS (root mean square) of Delta-DOR delay are 3.7 ns and 0.83 ns for s8525b and s8524b respectively. The corresponding RMS of range are 4.5 m and 0.5 m in the two individual observations. The difference between antenna apertures of Jiamusi and Qingdao is the main cause of RMS difference of range (Cao et al., 2016).

In s7912a, the STD of residuals is at the level of 0.47 ns. The delay closure has a standard deviation of 88 ps. Cao et al. (2016) analysed the precise positioning of the Chang'E 3 lander soft landing, argued that the random noise of Delta-DOR delay was 0.33 ns. Chang et al. (2016) used the different lunar gravity field model to evaluate RMS of Delta-DOR delay, the RMS was 0.36 ns when spacecraft was on 100 km × 100 km lunar orbit, 0.6 ns on 100 km × 15 km lunar orbit. The accuracy of our measurement of Delta-DOR within the strong RFI is comparable to those obtained by previous works without RFI.

Chang'E 3 is not the only spacecraft that DOR signals interfered by data-transmission signal. Chang'E 5 includes the lander-ascentor assembly and the orbiter. Each spacecraft can transmit two series of DOR signals and one series of data-transmission signal. The former is used for spacecraft position determination and latter transferring onboard science data. The beasons of Chang'E 5 had been tested at different CVN stations. When DOR signals and data-transmission signal emitted meanwhile, DOR signals were interfered by the side lobes of data-transmission signal to different degrees (Zhang et al., 2016). Local correlation provides a solution to the extremely RFI contaminated DOR signals processing.

Besides SNR and spanned bandwidth of tones, the precision of Delta-DOR measurement also depends on the precision of the quasar delay measurement, and on knowledge of the quasar position, clock stability, instrumental phase response, and uncertainties in Earth platform models and transmission media delays.

7 Conclusions and outlook

In this paper, we firstly present the performance of local correlation on low-SNR and strongly RFI contaminated DOR with China's lunar spacecraft. The results are verified by

Table 3. Accuracy of Delta-DOR

Code	Baseline	Bandwidth (MHz)	P_{tone}/N_0 (dBHz)	Integration (s)	Expected (ns)	Computed (ns)
s8525b	BJ-KM	7.6	1.0, 12	20	4.34	7.84
s8525b	BJ-UR	7.6	1.0, 20	20	4.20	8.73
s8525b	BJ-TM	7.6	1.0, 14	20	4.28	8.29
s8525b	KM-UR	7.6	12, 20	20	1.27	3.31
s8525b	KM-TM	7.6	12, 14	20	1.50	3.40
s8525b	UR-TM	7.6	20, 14	20	1.05	3.08
s8524b	BJ-KM	7.6	14, 20	20	1.05	1.08
s8524b	BJ-UR	7.6	14, 25	20	0.97	1.01
s8524b	BJ-TM	7.6	14, 24	20	0.98	1.02
s8524b	KM-UR	7.6	20, 25	20	0.53	0.48
s8524b	KM-TM	7.6	20, 24	20	0.55	0.50
s8524b	UR-TM	7.6	26, 25	20	0.35	0.29
s7912a	SH,KM,UR	38.4	34	5	0.05	0.47

[a]Footnote text here.

Table 4. RMS of Delta-DOR delay and range

Code	Delta-DOR (ns)	Range (m)
s8525b	3.7	4.2
s8524b	0.83	0.5

[a]Footnote text here.

means of error analysis on the residuals after orbit determination and post-fit. The main points of this paper are summarized as follows:

a. The local correlation method can enchance low-SNR processing ability for CVN to as low as 15 dBHz for carrier and 1 dBHz for tones. The performance of the method strongly depends on P_{tone}/N_0. The computed delay STD of post-fit residuals is compatible at 3 sigma level with the theoretical spacecraft thermal noise. The RMS of Delta-DOR delay after orbit determination are 3.7 ns when P_{tone}/N_0 varied in the range of 1 dBHz $\sim$ 20 dBHz, 0.83 ns when P_{tone}/N_0 varied in the range of 14 dBHz $\sim$ 26 dBHz.

b. Local correlation provides a solution to the special strongly RFI contaminated DOR signals processing. The RFI is data-transmission signal transmitted from another transponder on spacecraft. Local correlation can extract residual frequency and phase of tones even though they are totally submerged by RFI. The precision of Delta-DOR with strong RFI keeps the same level of that without interference.

Acknowledgments

The research presented in this paper has been supported by the National Natural Science Foundation of China (U1831137, 11703070, 11973011, 11803070, 11903067, 11803069), CAS Key Technology Talent Program, Shanghai Leading Talents program.

The data in this paper is accessible at https://pan.cstcloud.cn/s/tWbmv9X2QZQ.

References

Border, J. S. (2014). 210 Delta Differential One-way Ranging. *Jet Propuls. Lab. Calif. Inst. Technol. Invent. Math.*, *210*, 5–810.

Cao, J., Zhang, Y., Hu, S., Huang, Y., & Chen, M. (2016). An analysis of precise positioning and accuracy of the CE-3 lunar lander soft landing. *Geomatics Inf. Sci. Wuhan Univ.*, *41*(2), 274–278.

CCSDS. (2013). DELTA-DOR TECHNICAL CHARACTERISTICS AND PERFORMANCE. In *Rep. concern. sp. data syst. stand.* (pp. 1–67). Washington, DC, USA.

Chang, S., Huang, Y., Li, P., & Hu, X. (2016). Analysis on orbit determination of CE-3 with different lunar gravity field model. *Geomatics Inf. Sci. Wuhan Univ.*, *41*(11), 1427–1439.

Curkendall, D. W., & Border, J. S. (2013). Delta-DOR: The One-Nanoradian Navigation Measurement System of the Deep Space Network — History, Architecture, and Componentry. *Int. J. Mol. Sci.*, *14*(11), 23160–23187.

Duev, D. A., Pogrebenko, S. V., Cimò, G., Molera Calvés, G., Bocanegra Bahamón, T. M., Gurvits, L. I., ... Witasse, O. (2016). Planetary Radio Interferometry and Doppler Experiment (PRIDE) technique: A test case of the Mars Express Phobos fly-by. *Astron. Astrophys.*, *593*, 1–10. doi: 10.1051/0004-6361/201628869

Iess, L., & Ardito, R. A. P. A. (2006). THE EUROPEAN ΔDOR CORRELATOR. In (pp. 1–12). Valencia,Spain: 57th International Astronautical Congress.

James, N., Abello, R., Lanucara, M., Mercolino, M., & Maddè, R. (2009). Implementation of an ESA delta-DOR capability. *Acta Astronaut.*, *64*(11-12), 1041–1049. doi: 10.1016/j.actaastro.2009.01.005

Kinman, P. W., Bedrossian, A., Border, J. S., & Shin, D. (2015). Delta Differential One-way Ranging. *DSN Telecommun. Link Des. Handb.*, 1–25.

Rogstad, S. P., Jongeling, A. P., Finley, S. G., & White, L. A. (2009). DSN Beowulf Cluster-Based VLBI Correlator. *NASA Tech Briefs*, *33*(5), 58–59.

Wu, W., Wang, G., Jie, D., Zhang, X., & Jiang, D. (2013). High-accuracy VLBI technique using DOR signals. *Sci. Sin. Informationis*, *43*(2), 185–196. doi: 10.1360/112012-377

Wu, Y. (2009). *The design and implementation of key IP Cores in Chinese VLBI Data Acqusition System(CDAS)*. Unpublished doctoral dissertation.

Zhang, Z., Wang, J., Wang, G., & Ma, M. (2016). *Reports of the Docking experiments of Chang'E 5 beacons at VLBI stations* (Tech. Rep.). Shanghai Astronomical Observatory, Chinese Academy of Science.

Zheng, W., Tong, F., Zhang, J., Liu, L., & Shu, F. (2017). Interferometry imaging technique for accurate deep-space probe positioning. *Adv. Sp. Res.*, *60*(12), 2847–2854. Retrieved from `https://doi.org/10.1016/j.asr.2017.09.004` doi: 10.1016/j.asr.2017.09.004

Zheng, W., Zhang, J., Yu, Y., & Wang, W. (2014). Software correlator in the Chang'E 3 mission. IVS proceeding.